

Aging Effect on Microstructure and Machinability of Corrax Steel

Ahmet Serdar Guldibi

Faculty of Technology
Karabuk University
Karabuk, Turkey
aserdarguldibi@karabuk.edu.tr

Halil Demir

Faculty of Technology
Karabuk University
Karabuk, Turkey
hdemir@karabuk.edu.tr

Abstract—In this paper, the influence of the aging process on the microstructure and machinability of Corrax Steel was investigated for four samples: a solution heat-treated (A0) and three samples aged at 400°C (A4), 525°C (A5.25) and 600°C (A6) for four hours. The effect of aging temperature on hardness was examined. Machining tests were carried out using a CNC lathe with a multi-layer coated PVD (AlTiN) cutting tool, at various cutting speeds (50, 100, 150, 200, 250, 300, 350m/min) with constant feed rate (0.1mm/rev) and 1mm constant cutting depth. The microstructure was investigated using an optical microscope and EDS attached SEM. The effect of aging on reverted austenite formation was also evaluated. In order to understand the changes in surface topology, cutting forces and vibrations were measured. With increasing aging temperature, the lath martensite was transformed to plate martensite because of the formation of precipitates and reverted austenite. Aging at different temperatures increased hardness up to 58%, cutting forces up to 117% and surface roughness up to 450%. The results describe the effect of the aging treatment on cutting forces, surface topology, tool wear and vibrations.

Keywords—dry turning; corrax; cutting force, surface roughness; vibration

I. INTRODUCTION

Investigation of martensitic steels started in USA during the 60's. Martensitic steels have low carbon and have high strength and corrosion resistance [1]. These properties are reached by convenient composition and properly applied aging treatments. Corrax is a maraging steel appropriate for many applications such as plastics processing, extrusion dies, plastic extruder's screws, guideways, landing gears, dental, and medical equipment [2-4]. The main goal of manufacturing companies is advanced productivity, improving surface finish and dimensional precision while reducing cost [5]. However, these goals are difficult to achieve especially during machining, as hardened maraging steels are as hard to machine materials [6]. Cutting forces, specific cutting energy, shear angle, shear stress, friction coefficient and shear stress rates for AISI 420 steel at various cutting conditions and with various cutting tools have been investigated. According to test results, feed rate effects cutting forces, while cutting speed is the major effect of energy consumption. In [7], cutting forces and cutting energy reached maximum value at 60m/min and were reduced at

higher cutting speeds. The machining of PH 15-5 maraging steel, aged at 482°C to receive peak hardness value, was investigated in [8]. The machining tests were carried out using TiAlN coated tungsten carbide inserts with various nose radiuses (0.4, 0.8 and 1.2mm) at different cutting speeds and feed rates. Increasing feed rate increased cutting forces: 0.8mm nose radius caused higher cutting forces than 0.4mm and 1.2mm. High cutting speed, low feed rate and middle tool nose (0.8mm) generated minimum surface roughness value (0.447 μ m). The heat formation during hard turning of chromium hardfacing materials was studied in [9]. Results showed that increasing cutting speed or feed rate increased cutting temperature. The temperature increase rates depended on the microstructure of the material. Machining finer structures cause higher temperature increment rate. The predicted temperature for fine structured materials is 650-700°C, while for coarser structured materials is 600°C. The temperature and cutting forces during machining of SAE 4140 steel was investigated in [10]. Results showed that increasing cutting speed increases the temperature on the rake face, enlarging the tool-chip contact area.

The effects of hot turning on cutting forces, tool wear and surface topology, were examined in [11]. Experiments were carried out at room temperature, 300°C and 600°C. The outcomes showed that the increase of temperature decreased cutting forces, reduced tool wear, and improved surface topology. Machining Monel 400 at room temperature caused BUE formation, which enhanced tool's life compared to Inconel 625 and Inconel 718. BUE formation increased tool's life but also increased the surface roughness in the machining of Monel 400. Hot turning enhanced tool's life, but this enhancement was poor for Inconel 625 and Monel 400 compared to Inconel 718. The effects of different types of cutting fluid on cutting temperature, chip thickness, surface roughness, cutting forces and shear angle were investigated in [12]. Experiments were carried out under dry, conventional cutting fluid and cryogenic carbon dioxide at three different cutting speeds and four feed rates at 1mm cutting depth. Results showed that breakability was improved under cryogenic machining chips when compared to wet and dry machining. CO₂ penetrated better the cutting zone improving lubrication. Improved lubrication reduced the cutting temperature and cut chip thickness. Increasing cutting speed

decreased cutting forces because of the heat generated on the cutting zone. Under cryogenic cutting conditions, increasing cutting speed caused higher decrease in cutting forces, because of the improved lubrication. Increased cutting speed reduced surface roughness, cutting forces and vibration during machining. Increased feed rates also increased the surface roughness.

There are several researches about the aging treatment, strength, hardness, fracture toughness, strength in high temperature, reverted austenite formation, and hydrogen embrittlement of maraging steels [13-16]. However, there is a lack of extensive study on the machining of Corrax steel. This study investigated the machinability of solution heat treated and aged at three different conditions Corrax steel, under different cutting speeds, in order to understand the effect of aging on its microstructure, hardness, and machinability.

II. EXPERIMENTAL PROCEDURE

A. Workpiece Materials

Corrax steel was obtained from Uddeholm Turkey Corporation. The samples were solution heat treated at 850°C for 0.5h and subsequently air-cooled. Table I shows the chemical composition of steel, analyzed by the GNR Atlantis optical emission spectrometry.

TABLE I. CHEMICAL COMPOSITION OF CORRAX STEEL

Element	C	Si	Mn	P	S
%	0.048	0.203	0.253	0.012	0.026
Element	Cr	Mo	Ni	Al	
%	12.24	1.388	9.064	1.582	

B. Heat Treatment and Microstructure

The supplied Corrax steel had 350mm length and 35mm diameter. Four samples were obtained for the aging treatment. The samples were solution heat treated at 850°C for 0.5h and then cooled at room temperature before the aging treatment. After the solution heat treatment all samples, except one (A0), were aged at three different temperatures (400, 525, 600°C) for four hours and cooled in room temperature. At the end of the aging treatment, four sets of samples were obtained: (i) solution heat treated (A0), (ii) aged at 400°C (A4), (iii) aged at 525°C (A5.25) and (iv) aged at 600°C (A6). Conventional metallographic methods such as grinding, polishing and etching were used for microstructural investigation. Kalling's reagent was used for etching at various etching times, depending on material's hardness. Etching time depended on the hardness of each sample. The microstructure of the samples was examined using a Nikon Epiphot 200 optical microscope and an EDS equipt Carl Zeiss Ultra Plus Gemini Fesem scanning electron microscopy (SEM). XRD investigations were carried out using a Rigaku Ultima IV. XRD, SEM and EDS examinations were carried out in Iron and Steel Institute (MARGEM) at Karabuk University. Microhardness testing was conducted using a Shimadzu Vickers microhardness testing machine, with an HV1 (9,807N) load and 15s holding time. At minimum five hardness measurements were made on each sample and their average was accepted as hardness value.

C. Machine and Cutting Tool

Machining tests were accomplished using a Fanuc Control unit equipped with a Johnford TC-35 Lathe having 10KW power. The turning tests were carried out using PVD multilayer-coated cementite carbide inserts with a CNMG120408RP geometry. The cutting inserts were designed by Kennametal. The inserts were mechanically fixed on a tool holder with a DCLNR2525 geometry. The inserts were designated by KC5010 Kennametal which is equivalent to P10-20.

D. Cutting Parameters

Machining tests were performed under dry cutting conditions without any cooling liquid. Cutting parameters were determined into the recommended, by the manufacturer, limits in order to observe the performance of the cutting inserts. The cutting parameters are exposed in Table II.

TABLE II. CUTTING PARAMETERS

Workpiece samples	Vc (m/min)	f (mm/rev)	ap (mm)
A0 A4 A5.25 A6	50	0.1	1
	100		
	150		
	200		
	250		
	300		
	350		

Cutting forces were measured using Kistler 9257B piezoelectric 3-axes dynamometer. The Mitutoyo SurfTest 211 surface roughness tester was used for measuring the surface roughness. Three different measurements were made on each surface and their average was accepted as the surface roughness value. Vibration measurements were performed using iDynamic application [17] with an MTK sensor having 0.00390625 m/s² resolution.

III. RESULTS AND DISCUSSION

A. Workpiece Materials

Optical micrographs of A0, A4, A5.25 and A6 are shown in Figure 1, while similar microstructure investigations for PH 13-8 Mo were carried out in [18, 19]. As it can be observed, the microstructure of the sample A0 has large and irregular massive martensite blocks. Increasing aging temperature transforms the martensite structure from lath to plate. While massive martensite structures are seen in Figure 1(a)-1(c), Figure 1(d) shows the plate martensite structure. Figure 1(c) shows the microstructure of the A5.25 sample with molybdenum carbides in the aged martensite structure [20]. The martensitic structure is smaller, compared to A0 and A4 samples. The microstructure of the A6 sample, seen in Figure 1(d), has the highest amount of reverted austenite, indicated by white areas [21]. The transformation of massive to plate martensite with the increase of aging temperature can be explained by the formation of reverted austenite on the martensite borders [15, 22]. The growth of reverted austenite into martensite reduced massive martensite to plate martensite. In addition, the Al content allows NiAl precipitations through aging which caused resistance to coarsening, even at high temperatures [23].

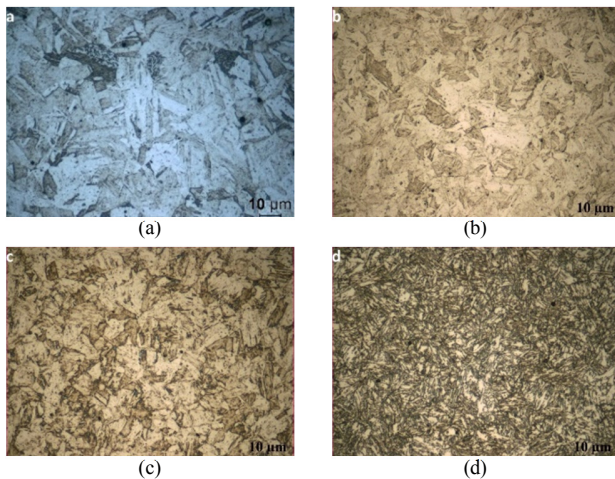


Fig. 1. Microstructure of: a) solution heat treated (A0), b) aged at 400°C (A4), c) aged at 525°C (A5.25). d) aged at 600°C (A6)

Maraging steels are designed to form a martensitic structure and austenite transforms completely into martensite during cooling [29-32]. The XRD patterns of the samples, presented in Figure 2, indicate that the dominant microstructure consisted of martensite phase. The significant intensity peaks of bcc(110) with small intensity of bcc(200) and bcc(211) show the martensite phase formation. The aging treatment causes a reverted austenite formation in the microstructure. Increasing the aging temperature also increases the amount of reverted austenite in the microstructure, as seen in Figure 2.

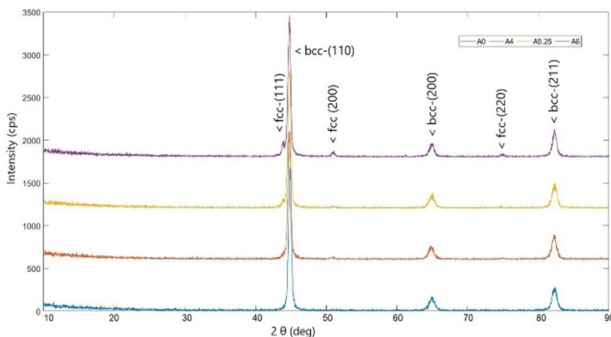


Fig. 2. XRD patterns of samples

Figure 3 shows the EDS analysis with the spectrum points 1-6 white marked on the microstructure of the A5.25 sample. The selected points contain different percentages of C, Cr, Ni, Mn, Fe and Al elements. The existence of these elements demonstrates a small amount of NiAl, CrC, MoC, Fe₃C and NiMn precipitates, which affect the strength of steels [13, 24-26]. The precipitations in the martensite structure hinders the dislocation motion that enhances the strength of steel [27, 28]. Aging at temperatures over 525°C causes a significant amount of reverted austenite [14]. Reverted austenite nucleates at the martensite lath boundary and low amounts of reverted austenite are not visible under a light microscope [33]. This austenite formation is the result of an uncompleted transformation of austenite into martensite. The aging process causes an inverse

transformation from martensite to austenite [34, 35], while similar results were reported for Corrax [36, 37]. The solution heat treated sample (A0) has less than 2% retained austenite [38]. Increasing aging temperature and time, increased the reverted austenite formation [39, 40]. Retained austenite, which is free of precipitates, decreased toughness and strength as reported in [41]. The reason for this decrease in toughness and strength can be explained by the brittle character of the matrix, in which the overaged particles serve as crack nucleation sites [42-44].

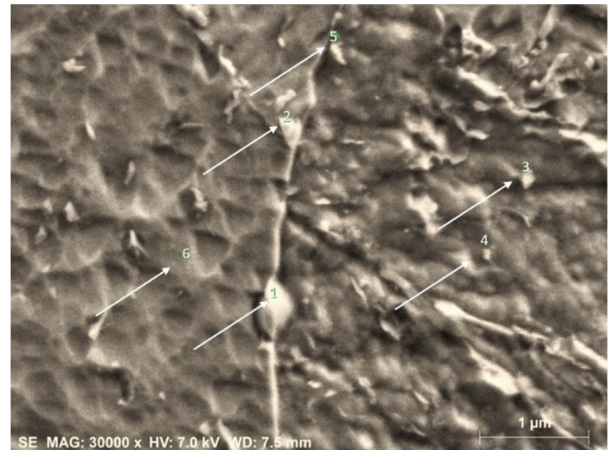


Fig. 3. SEM Image of A5.25 sample aged at 525°C

TABLE III. EDS OF INDICATED PARTICLES IN A5.25

Spectrum	C	Al	Cr	Mn	Fe	Ni	Mo
1	17.22	1.35	20.20	2.11	51.72	6.26	1.14
2	6.95	1.11	23.16	2.82	54.00	10.64	1.32
3	2.07	1.88	19.11	6.01	60.49	9.14	1.30
4	2.74	1.54	19.17	3.81	62.13	9.50	1.12
5	3.89	1.55	18.67	1.02	62.50	11.19	1.19
6	2.50	1.48	18.83	4.41	62.43	9.89	0.46
Mean value	5.89	1.49	19.86	3.36	58.88	9.44	1.09
Sigma	5.82	0.25	1.71	1.77	4.77	1.73	0.32
Sigma mean	2.38	0.10	0.70	0.72	1.95	0.71	0.13

B. Micro Hardness

Micro hardness tests were carried out at room temperature and the results are shown in Figure 4. Hardness was affected by aging temperature. The lowest hardness was measured for the A0 sample. Increasing aging temperature up to 525°C increased hardness and its highest value was obtained at aging temperature of 525°C. The increase on hardness can be explained by the diffusion assisted mechanism that hinders the dislocation movements. The principle of the particle strengthening is hindered by the dislocation movement of nanometer-sized particles precipitation [45, 46]. Higher aging temperatures decrease hardness, because of the growth of precipitations and reverted austenite formation in the microstructure [16, 47-49].

C. Cutting Forces

Turning experiments were carried out at seven different cutting speeds (50, 100, 150, 200, 250, 300, 350m/min), at a constant feed rate of 0.1mm/rev and 1mm cutting depth.

Cutting forces are shown in Figure 5. Aged samples cause higher cutting forces than the solution heat treated sample A0, e.g. the cutting forces increased by 85% for A4, 103% for A5.25 and 96% for A6 samples respectively, compared to those of the A0 sample. The highest cutting force was measured during the machining of the A5.25 sample, which is attributed to its highest material hardness. The lowest cutting force was measured in A0, which had the lowest hardness (332Hv). The results showed that the aging treatment has a great influence on cutting forces because of the precipitation formation in the microstructure. Precipitations hinder the movement of dislocations, reducing the cutting forces increment. However, overaging causes a decrease of cutting forces and hardness because of the overgrowth of precipitations. These reasons explain the decrease of cutting forces during the machining of the A6 sample.

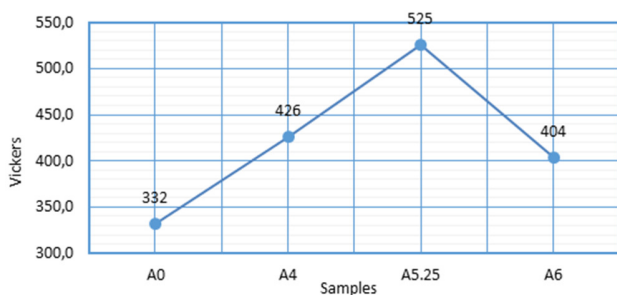


Fig. 4. Hardness of the samples

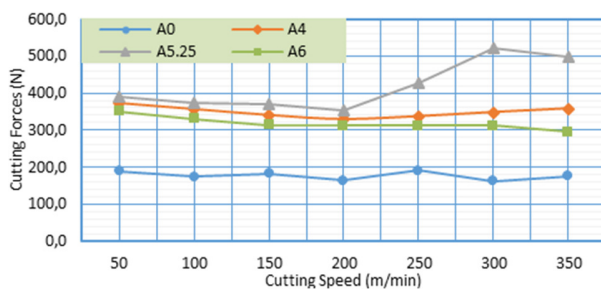


Fig. 5. Cutting forces versus cutting speed

The effect of cutting speed on the cutting forces was also investigated for each sample. The lowest cutting forces were measured at 200m/min, for all samples with the exception of A6. The lowest cutting forces for A6 sample were obtained at 350m/min. Machining A0 sample at different cutting speeds caused irregular cutting forces, which can be attributed to vibrations as seen in Figure 6 [50]. The cutting forces of aged samples, except from A5.25 decrease for cutting speeds up to 200m/min. This can be explained by the temperature increments on the cutting zone [51]. While machining materials harder than 45HRc (hard turning) the temperature on the cutting zone reaches an austenization temperature softening the material while machining [52-56]. Machining of A5.25 caused high cutting forces at cutting speeds higher than 200m/min because of serious tool wear. Tool wear changes the shape of the rake angle and the tool-chip interface. A small decrease at 350m/min can be noted in Figure 5. This can be explained by the extreme tool wear, as seen in Figure 7, which changes the

cutting depth. The cutting forces depend on the material's hardness: increasing hardness increases cutting forces. The A6 sample has the lowest cutting forces, compared to the other samples. This can be explained by its lowest hardness value and the retained austenite formation in its microstructure. Retained austenite decreases strength and hardness. In general, increasing cutting speed decreases cutting forces. This can be explained by the decreased on tool-chip interface and the increased heat on cutting zone that soften shear strength [57].

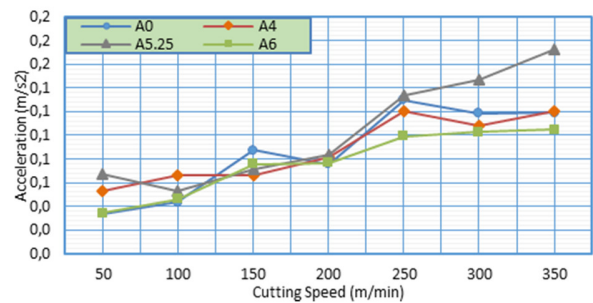


Fig. 6. Root mean square values at different cutting forces

Tool wear changes tool's geometry, affecting the cutting process. This is the reason why cutting forces and vibrations are high at excessive cutting speeds, as seen in Figures 5 and 6. A small increment of vibrations, as seen in Figure 6 at 150m/min cutting speed for A0, can be explained by the continuous chip formation. The increment of vibrations at 150m/min caused the increase of cutting forces. The lowest vibrations were measured in the A6 sample, which can be explained by the reverted austenite in the microstructure that reduced hardness and toughness. As a result, it can be noted that vibrations have great effect on cutting forces.

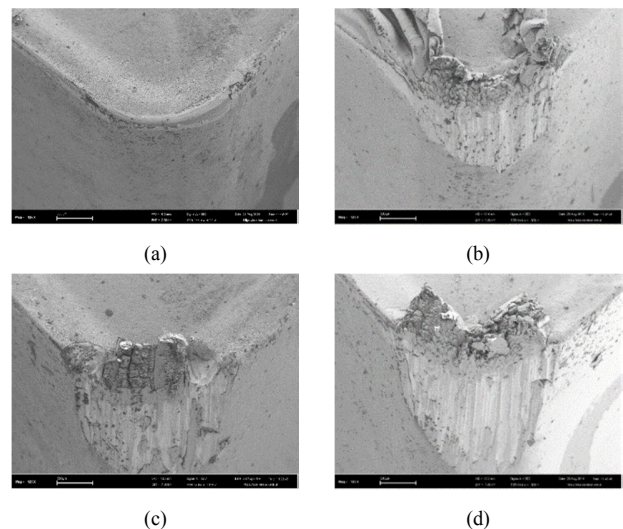


Fig. 7. SEM images of worn cutting tools for A5.25 samples after machining at: a) 200m/min, b) 250m/min, c) 300m/min, and d) 350m/min

D. Surface Roughness

Figure 8 shows the workpiece surface roughness values for A0 (332Hv), A4 (426Hv), A5.25 (525Hv) and A6 (404Hv)

samples. The measured surface roughness value for each sample is the average of three measurements. Cutting speed has great influence on the produced surface roughness. Increasing cutting speed decreases surface roughness. However, increasing cutting speed for the hardest sample, A5.25, caused serious tool wear, which disrupted the surface topology. Machining of the A0 and A6 samples showed the lowest surface roughness. This is explained by the lowest hardness value of A0 and the reverted austenite formation in the microstructure of A6, which decreased toughness and hardness. Low hardness and toughness ease the cutting process, enhancing surface roughness.

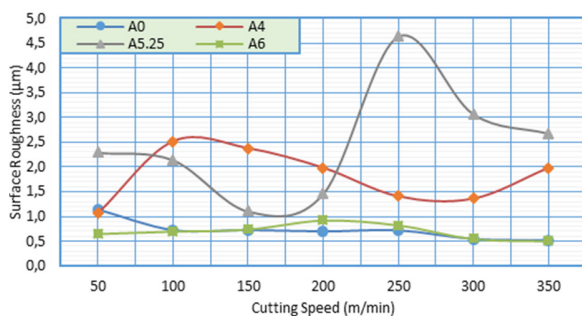


Fig. 8. Surface roughness versus cutting speed

Machining A0 at a 50m/min cutting speed showed an increase of surface roughness comparing to the A6 sample. This is explained by the continuous chip formation, as seen in Figure 9, which damaged the machined surface.

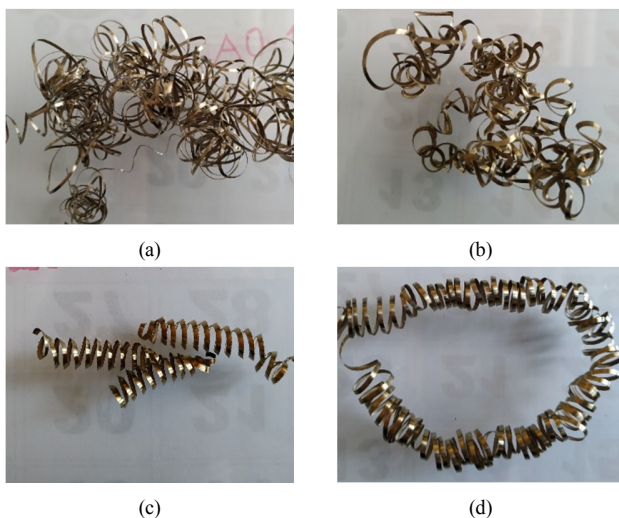


Fig. 9. Chip formation at 50m/min for: a) A0, b) A4, c) A5.25, and d) A6

The lowest surface roughness was obtained at 350m/min, as $0.51\mu\text{m}$ for both A0 and A6 samples. However, surface roughness values for the A4 sample were not usual. The peak surface roughness value for A4 sample was obtained at a 100m/min cutting speed, which is explained by the vibration peak, as it can be noted in Figure 6 [58]. Machining A5.25 (525Hv) at 50m/min caused a tool overhang and the highest vibration, as it can be noted in Figure 6, being the reason of the

high surface roughness [59]. Extreme high surface roughness values for A5.25 were obtained at 250, 300 and 350m/min cutting speeds because of serious tool wear, which also caused vibrations, as it can be noted in Figure 6. As a conclusion, the vibration has great effect on surface topology. There are many reasons for cutting forces and surface roughness correlation. One of the main is the effect of the vibrations while machining. The rise of vibrations depends on cutting speed, tool wear, and the samples' microstructure. The increase of vibrations caused an increase of cutting forces. Serious tool wear also increased vibration formation. The lowest vibrations were obtained during the machining of the A6 sample, something that can be explained by the reverted austenite formation that reduced hardness and toughness.

IV. CONCLUSION

This study investigated the influence of precipitation and reverted austenite formation on cutting forces and surface roughness of Corrax steel. Machining tests were carried out for A0 (332Hv), A4 (426Hv), A5.25 (525Hv) and A6 (404Hv) samples. The results showed that:

- The aging treatment has a major effect on the formation of precipitation that causes an increase on hardness. The highest hardness was measured for the sample aged at 525°C for four hours. Hardness increase is a result of precipitation formation in the microstructure. Aging temperatures higher than 525°C decreased hardness due to overaging which caused reverted austenite formation and the growth of precipitations in the microstructure.
- Aging treatment improves the mechanical properties and makes the cutting process more difficult. Machining of the hardest sample (A5.25) caused serious tool wear at high cutting speeds such as 250, 300 and 350 m/min. Cutting forces were increased by sample's aging temperature up to 525°C . Aging at 600°C caused a cutting forces decrease because of the reverted austenite formation and the growth of precipitations.
- Cutting speed, vibration and tool wear affected seriously surface roughness. The lowest surface roughness values were measured for A0 and A6 samples. Vibration and tool wear have a serious effect on the surface roughness values, as well as cutting forces. Reverted austenite formation also reduced vibrations and improved surface roughness.

ACKNOWLEDGMENT

This research was supported by the Scientific Research Projects Department of Karabuk University (BAP) with Project No KBÜBAP-18-KP-145.

REFERENCES

- [1] L. W. Tsay, H. H. Chen, M. F. Chiang, C. Chen, "The influence of aging treatments on sulfide stress corrosion cracking of PH 13-8 Mo steel welds", *Corrosion Science*, Vol. 49, No. 6, pp. 2461–2473, 2007
- [2] C. Zheng, R. Schoell, P. Hosemann, D. Kaoumi, "Ion irradiation effects on commercial PH 13-8 Mo maraging steel Corrax", *Journal Of Nuclear Materials*, Vol. 514, pp. 255–265, 2019
- [3] Z. Guo, W. Sha, D. Vaumousse, "Microstructural evolution in a PH13-8 stainless steel after ageing", *Acta Materialia*, Vol. 51, No. 1, pp. 101–116, 2003

- [4] G. Pantazopoulos, T. Papazoglou, P. Psyllaki, G. Sfantos, S. Antoniou, K. Papadimitriou, J. Sideris, "Sliding wear behaviour of a liquid nitrocarburised precipitation-hardening (PH) stainless steel", *Surface and Coatings Technology*, Vol. 187, No. 1, pp. 77–85, 2004
- [5] V. Varghese, K. Akhil, M. R. Ramesh, D. Chakradhar, "Investigation on the performance of AlCrN and AlTiN coated cemented carbide inserts during end milling of maraging steel under dry, wet and cryogenic environments", *Journal Of Manufacturing Processes*, Vol. 43, No. A, pp. 136–144, 2019
- [6] A. Kumar, Y. Balaji, N. E. Prasad, G. Gouda, K. Tamilmani, "Indigenous development and airworthiness certification of 15–5 PH precipitation hardenable stainless steel for aircraft applications", *Sadhana*, Vol. 38, No. 1, pp. 3–23, 2013
- [7] A. M. El-Tamimi, T. M. El-Hossainy, "Investigating the machinability of AISI 420 stainless steel using factorial design", *Materials and Manufacturing Processes*, Vol. 23, No. 4, pp. 419–426, 2008
- [8] D. Palanisamy, P. Senthil, V. Senthilkumar, "The effect of aging on machinability of 15Cr–5Ni precipitation hardened stainless steel", *Archives of Civil and Mechanical Engineering*, Vol. 16, No. 1, pp. 53–63, 2016
- [9] X. J. Ren, Q. X. Yang, R. D. James, L. Wang, "Cutting temperatures in hard turning chromium hardfacings with PCBN tooling", *Journal of Materials Processing Technology*, Vol. 147, No. 1, pp. 38–44, 2004
- [10] N. A. Abukhshim, P. T. Mativenga, M. A. Sheikh, "Investigation of heat partition in high speed turning of high strength alloy steel", *International Journal of Machine Tools and Manufacture*, Vol. 45, No. 15, pp. 1687–1695, 2005
- [11] A. K. Parida, K. Maity, "Comparison the machinability of Inconel 718, Inconel 625 and Monel 400 in hot turning operation", *Engineering Science and Technology, an International Journal*, Vol. 21, No. 3, pp. 364–370, 2018
- [12] B. D. Jerold, M. P. Kumar, "Experimental investigation of turning AISI 1045 steel using cryogenic carbon dioxide as the cutting fluid", *Journal of Manufacturing Processes*, Vol. 13, No. 2, pp. 113–119, 2011
- [13] A. M. Patel, R. W. Neu, J. A. Pape, "Growth of small fatigue cracks in PH 13-8 Mo stainless steel", *Metallurgical and Materials Transactions A*, Vol. 30, No. 5, pp. 1289–1300, 1999
- [14] V. Seetharaman, M. Sundararaman, R. Krishnan, "Precipitation hardening in a PH 13-8 Mo stainless steel", *Materials Science and Engineering*, Vol. 47, No. 1, pp. 1–11, 1981
- [15] X. Li, J. Zhang, J. Chen, S. Shen, G. Yang, T. Wang, X. Song, "Effect of aging treatment on hydrogen embrittlement of PH 13-8 Mo martensite stainless steel", *Materials Science And Engineering: A*, Vol. 651, pp. 474–485, 2016
- [16] R. Schnitzer, G. A. Zickler, E. Lach, H. Clemens, S. Zinner, T. Lippmann, H. Leitner, "Influence of reverted austenite on static and dynamic mechanical properties of a PH 13-8 Mo maraging steel", *Materials Science and Engineering: A*, Vol. 527, No. 7–8, pp. 2065–2070, 2010
- [17] A. Feldbusch, H. Sadegh-Azar, P. Agne, "Vibration analysis using mobile devices (smartphones or tablets)", *Procedia Engineering*, No. 199, pp. 2790–2795, 2017
- [18] S. P. Bruhl, R. Charadia, S. Simison, D. G. Lamas, A. Cabo, "Corrosion behavior of martensitic and precipitation hardening stainless steels treated by plasma nitriding", *Surface and Coatings Technology*, Vol. 204, No. 20, pp. 3280–3286, 2010
- [19] Z. Huang, M. D. Abad, J. K. Ramsey, M. R. de Figueiredo, D. Kaoumi, N. Li, M. Asta, N. Gronbeck-Jensen, P. Hosemann, "A high temperature mechanical study on PH 13-8 Mo maraging steel", *Materials Science and Engineering: A*, Vol. 651, pp. 574–582, 2016
- [20] L. C. da Silva, P. R. da Mota, M. B. da Silva, W. F. Sales, A. R. Machado, M. J. Jackson, "Burr height minimization using the response surface methodology in milling of PH 13-8 Mo stainless steel", *International Journal of Advanced Manufacturing Technology*, Vol. 87 No. 9–12, pp. 3485–3496, 2016
- [21] M. M. A. Bepari, "Carburizing: A Method of Case Hardening of Steel", *Comprehensive Materials Finishing*, Vol. 2, pp. 71–106, 2017
- [22] M. Farooque, H. Ayub, A. Ul Haq, A. Q. Khan, "The formation of reverted austenite in 18% Ni 350 grade maraging steel", *Journal of Materials Science*, Vol. 33, No. 11, pp. 2927–2930, 1998
- [23] Y. Snir, S. Haroush, A. Danon, A. Landau, Y. Gelbstein, D. Eliezer, "Metallurgical and hydrogen effects on the small punch tested mechanical properties of PH-13-8Mo stainless steel", *Materials*, Vol. 11, No. 10, Article ID 1966, 2018
- [24] Z. B. Jiao, J. H. Luan, M. K. Miller, Y. W. Chung, C. T. Liu, "Co-precipitation of nanoscale particles in steels with ultra-high strength for a new era", *Materials Today*, Vol. 20, No. 3, pp. 142–154, 2017
- [25] R. Schnitzer, R. Radis, M. Nohrer, M. Schober, R. Hochfellner, S. Zinner, E. Povoden-Karadeniz, E. Kozeschnik, H. Leitner, "Reverted austenite in PH 13-8 Mo maraging steels", *Materials Chemistry and Physics*, Vol. 122, No. 1, pp. 138–145, 2010
- [26] M. Murayama, K. Hono, Y. Katayama, "Microstructural evolution in a 17-4 PH stainless steel after aging at 400 °C", *Metallurgical and Materials Transactions A*, Vol. 30, No. 2, pp. 345–353, 1999
- [27] M. Elitas, B. Demir, "The effects of the welding parameters on tensile properties of RSW junctions of DP1000 sheet steel", *Engineering, Technology & Applied Science Research*, Vol. 8, No. 4, pp. 3116–3120, 2018
- [28] L. Carneiro, B. Jalalahmadi, A. Ashtekar, Y. Jiang, "Cyclic deformation and fatigue behavior of additively manufactured 17–4 PH stainless steel", *International Journal of Fatigue*, Vol. 123, pp. 22–30, 2019
- [29] C. M. Wayman, "Martensitic transformations and mechanical behavior", 7th International Conference on the Strength of Metals and Alloys, Montreal, Canada, August 12–16, 1985
- [30] E. V. Pereloma, A. Shekhter, M. K. Miller, S. P. Ringer, "Ageing behaviour of an Fe–20Ni–1.8Mn–1.6Ti–0.59Al (wt%) maraging alloy: clustering, precipitation and hardening", *Acta Materialia*, Vol. 52, No. 19, pp. 5589–5602, 2004
- [31] K. Nagayama, T. Terasaki, K. Tanaka, F. D. Fischer, T. Antretter, G. Cailletaud, F. Azzouz, "Mechanical properties of a Cr–Ni–Mo–Al–Ti maraging steel in the process of martensitic transformation", *Materials Science and Engineering: A*, Vol. 308, No. 1–2, pp. 25–37, 2001
- [32] S. Floreen, "The physical metallurgy maraging steels", *Metallurgical Reviews*, Vol. 13, No. 1, pp. 115–128, 1969
- [33] N. Atsmon, A. Rosen, "Reverted austenite in maraging steel", *Metallography*, Vol. 14, No. 2, pp. 163–167, 1981
- [34] N. El-Bagoury, M. M. Hessien, Z. I. Zaki, "Influence of aging on microstructure, martensitic transformation and mechanical properties of NiTiRe shape memory alloy", *Metals and Materials International*, Vol. 20, No. 6, pp. 997–1002, 2014
- [35] L. T. Shiang, C. M. Wayman, "Maraging behavior of an Fe-19.5Ni-5Mn alloy II: Evolution of reverse-transformed austenite during overaging", *Metallography*, Vol. 21, No. 4, pp. 425–451, 1988
- [36] R. B. Frandsen, T. Christiansen, M. A. J. Somers, "Simultaneous surface engineering and bulk hardening of precipitation hardening stainless steel", *Surface and Coatings Technology*, Vol. 200 No. 16–17, pp. 5160–5169, 2006
- [37] A. K. Jahja, P. Parikin, N. Effendi, "The influence of heat treatment time and temperature on the physical properties of assab-corax steel", *Atom Indonesia*, Vol. 31, No. 2, pp. 91–102, 2005
- [38] S. Horing, D. Abou-Ras, N. Wanderka, H. Leitner, H. Clemens, J. Banhart, "Characterization of reverted austenite during prolonged ageing of maraging steel CORRAX", *Steel Research International*, Vol. 80, No. 1, pp. 84–88, 2009
- [39] U. K. Viswanathan, S. Banerjee, R. Krishnan, "Effects of aging on the microstructure of 17-4 PH stainless steel", *Materials Science and Engineering: A*, Vol. 104, pp. 181–189, 1988
- [40] C. N. Hsiao, C. S. Chiou, J. R. Yang, "Aging reactions in a 17-4 PH stainless steel", *Materials Chemistry and Physics*, Vol. 74, No. 2, pp. 134–142, 2002
- [41] C. A. Pampillo, H. W. Paxton, "The effect of reverted austenite on the mechanical properties and toughness of 12 Ni and 18 Ni (200) maraging steels", *Metallurgical and Materials Transactions B*, Vol. 3, No. 11, pp. 2895–2903, 1972

- [42] U. K. Viswanathan, G. K. Dey, V. Sethumadhavan, "Effects of austenite reversion during overageing on the mechanical properties of 18 Ni (350) maraging steel", *Materials Science and Engineering: A*, Vol. 398, No. 1-2, pp. 367-372, 2005
- [43] C. R. Shanthan, R. Narayanan, K. J. L. Iyer, V. M. Radhakrishnan, S. K. Seshadri, S. Sundararajan, S. Sundaresan, "Microstructural changes during welding and subsequent heat treatment of 18Ni (250-grade) maraging steel", *Materials Science and Engineering: A*, Vol. 287, No. 1, pp. 43-51, 2000
- [44] H. J. Rack, D. Kalish, "Strength and fracture toughness of 18 Ni (350) maraging steel", *Metallurgical and Materials Transactions B*, Vol. 2, No. 11, pp. 3011-3020, 1971
- [45] W. Sha, H. Leitner, Z. Guo, W. Xu, "Phase transformations in maraging steels", *Phase Transformations in Steels*, Vol. 2, pp. 332-362, 2012
- [46] S. M. Rajaa, H. A. Abdulhadi, K. S. Jabur, G. R. Mohammed, "Aging time effects on the mechanical properties of Al 6061-T6 alloy", *Engineering, Technology & Applied Science Research*, Vol. 8, No. 4, pp. 3113-3115, 2018
- [47] C. V. Robino, M. J. Cieslak, P. W. Hochanadel, G. R. Edwards, "Heat treatment of investment cast PH 13-8 Mo stainless steel: part II. isothermal aging kinetics", *Metallurgical and Materials Transactions A*, Vol. 25, No. 4, pp. 697-704, 1994
- [48] A. Polat, M. Avsar, F. Ozturk, "Effects of the artificial-aging temperature and time on the mechanical properties and springback behavior of AA6061", *Materials and Technology*, Vol. 49, No. 4, pp. 487-493, 2015
- [49] A. N. Singh, A. Moitra, P. Bhaskar, G. Sasikala, A. Dasgupta, A. K. Bhaduri, "Effect of thermal aging on microstructure, hardness, tensile and impact properties of Alloy 617", *Materials Science and Engineering: A*, Vol. 710, pp. 47-56, 2018
- [50] M. Kayhan, E. Budak, "An experimental investigation of chatter effects on tool life", *Proceedings of the Institution of Mechanical Engineers, Part B: Journal of Engineering Manufacture*, Vol. 223, No. 11, pp. 1455-1463, 2009
- [51] V. S. Sharma, S. Dhiman, R. Sehgal, S. K. Sharma, "Estimation of cutting forces and surface roughness for hard turning using neural networks", *Journal Of Intelligent Manufacturing*, Vol. 19, No. 4, pp. 473-483, 2008
- [52] W. Grzesik, "A revised model for predicting surface roughness in turning", *Wear*, Vol. 194, No. 1-2, pp. 143-148, 1996
- [53] H. Demir, S. Gunduz, "The effects of aging on machinability of 6061 aluminium alloy", *Materials & Design*, Vol. 30, No. 5, pp. 1480-1483, 2009
- [54] B. N. Pathak, K. L. Sahoo, M. Mishra, "Effect of machining parameters on cutting forces and surface roughness in Al-(1-2) Fe-1V-1Si alloys", *Materials and Manufacturing Processes*, Vol. 28, No. 4, pp. 463-469, 2013
- [55] L. Chen, B. L. Tai, R. G. Chaudhari, X. Song, A. J. Shih, "Machined surface temperature in hard turning", *International Journal of Machine Tools and Manufacture*, Vol. 121, pp. 10-21, 2017
- [56] P. Sivaiah, D. Chakradhar, "Modeling and optimization of sustainable manufacturing process in machining of 17-4 PH stainless steel", *Measurement*, Vol. 134, pp. 142-152, 2019
- [57] E. Trent, P. K. Wright, *Metal cutting*, Elsevier, 2000
- [58] S. S. Abuthakeer, P. V. Mohanram, G. Mohan Kumar, "The effect spindle vibration on surface roughness of workpiece in dry turning using Anova", *International Journal of Current Research and Review*, Vol. 3, No. 4, pp. 13-28, 2011
- [59] M. H. El-Axir, M. M. Elkhabeery, M. M. Okasha, "Modeling and parameter optimization for surface roughness and residual stress in dry turning process", Vol. 7, No. 5, pp. 2047-2055, 2017